Hard-to-soft transition-enhanced piezoelectricity in poly(vinylidene fluoride) via relaxor-like secondary crystals activated by high-power ultrasonication†

Guanchun Rui [a], Elshad Allahyarov [b,c,d], Ruipeng Li [e], Philip L. Taylor [b,*], Lei Zhu [a,*]

[a] *Department of Macromolecular Science and Engineering, Case Western Reserve University, Cleveland, Ohio 44106-7202, United States*

[b] *Department of Physics, Case Western Reserve University, Cleveland, Ohio 44106-7079, United States*

[c] *Institut für Theoretische Physik II: Weiche Materie, Heinrich-Heine Universität Düsseldorf, Universitätstrasse 1, 40225 Düsseldorf, Germany*

[d] *Theoretical Department, Joint Institute for High Temperatures, Russian Academy of Sciences, 13/19 Izhorskaya street, Moscow 125412, Russia*

[e] *National Synchrotron Light Source II, Brookhaven National Laboratory, Upton, New York 11973, United States*

† Electronic supplementary information (ESI) available. See DOI: XXX

* Corresponding authors. Emails: lxz121@case.edu (L. Zhu) and plt@case.edu (P.L. Taylor)

Abstract

Although high piezoelectric coefficients have recently been observed in poly(vinylidene fluoride-*co*-trifluoroethylene) [P(VDF-TrFE)] random copolymers, they have low Curie temperatures, which makes their piezoelectricity thermally unstable. It has been challenging to achieve high piezoelectric performance from the more thermally stable PVDF homopolymer. In this report, we describe how high-power ultrasonic processing was used to induce a hard-to-soft piezoelectric transition and improve the piezoelectric coefficient d_{31} in neat PVDF. After high-power ultrasonication for 20 min, a uniaxially stretched and poled PVDF film exhibited a high d_{31} of 50.2±1.7 pm/V at room temperature. Upon heating to 65 °C, the d_{31} increased to a maximum value of 76.2±1.2 pm/V, and the high piezoelectric performance persisted up to 110 °C. The enhanced piezoelectricity was attributed to the relaxor-like secondary crystals in the oriented amorphous fraction, broken off from the primary crystals by ultrasonication, as suggested by differential scanning calorimetry and broadband dielectric spectroscopy studies.

Keywords: Hard-to-soft piezoelectric transition, poly(vinylidene fluoride), ultrasonication, relaxor-like secondary crystals, oriented amorphous fraction

Introduction

For ceramic piezoelectrics, a hard piezoelectric has a relativity low dielectric constant and thus a low piezoelectric coefficient (e.g., d_{33} ~ 200 pC/N for neat lead titanate zirconate, PZT) with a linear electromechanical response (hysteresis < 2%). To enhance their piezoelectric coefficients, the hard-to-soft transition has been employed.[1] By chemical doping to facilitate domain wall motion and polarizability, a hard piezoelectric can be converted to a soft piezoelectric having a drastically enhanced dielectric constant and piezoelectricity (e.g., d_{33} ~ 600 pC/N for doped PZT) at the sacrifice of larger electromechanical hysteresis (~17%).[2, 3] This strategy, however, has never been realized for piezoelectric polymers, which have a good potential for flexible/wearable electronics and soft robotics. For example, typical piezoelectric coefficients (d_{31} and d_{33}) for poly(vinylidene fluoride) (PVDF) and its random copolymers, poly(VDF-*co*-trifluoroethylene) [P(VDF-TrFE)], are less than 35 pC/N, significantly lower than those of even hard ceramic piezoelectrics (Fig. S1, ESI†).

Much effort has been dedicated to enhancing the performance of piezoelectric polymers over the past decades, and various physical models have been proposed, such as the crystal/amorphous matrix composite model (or the dimensional effect),[4-9] the Poisson ratio effect from the amorphous phase orientation,[10] crystal actuation from conformational transformation,[11-13] and the amorphous-crystal interface contribution.[14, 15] However, a comprehensive understanding of the piezoelectric mechanism in semicrystalline polymers has not been achieved until recently. Liu *et al.* discovered a morphotropic phase boundary (MPB) behavior in P(VDF-TrFE) copolymers having a molar composition around 50/50.[12, 13] By utilizing the helical-to-all trans conformation transformation in the crystalline phase, a large d_{33} of ~63.5 pC/N was achieved in a P(VDF-TrFE) 50/50 mol% sample. On the other hand, P(VDF-TrFE) copolymers with a molar

composition above 65/35 exhibited low piezoelectric constants. Later, more details were found for uniaxially stretched P(VDF-TrFE) copolymers with a molar composition around 50/50.[16, 17] After thermal annealing in the paraelectric phase, extended-chain crystals (ECCs) were obtained, together with a significant amount (~25%) of oriented amorphous fraction (OAF) linking the ECCs to the isotropic amorphous fraction (IAF). Upon unipolar poling to induce macroscopic polarization of the sample, secondary crystals (SCs) grew in the OAF (denoted as SC_{OAF}). It was found that the conformation transformation from helical to all trans in the relaxor-like SC_{OAF} enhanced the piezoelectric coefficients to d_{31} ~ 77 pm/V and d_{33} ~ 69 pm/V for the low-VDF-content P(VDF-TrFE) copolymers (note, pC/N = pm/V, and in our study pC/N and pm/V are used for direct and inverse piezoelectric coefficients, respectively). However, these low-VDF-content P(VDF-TrFE) copolymers are of limited utility, as their piezoelectric performance vanishes above the low Curie transition temperatures (T_C) of ~65 °C (Fig. S1, ESI†).

In the quest for stable high-piezoelectric performance, it is therefore appropriate to focus on PVDF homopolymers or high-VDF-content P(VDF-TrFE) copolymers, as their working temperature limits can be much higher due to their high T_C [note that the T_C of PVDF is above its melting temperature (T_m) at ambient pressure[18]].[19, 20] By utilizing the OAF in biaxially oriented PVDF, a high direct d_{33} of 65 pC/N has been obtained.[21] However, no SC_{OAF} could be induced in PVDF homopolymers, because no ECCs can be obtained by crystallization under normal processing conditions (we do note that PVDF ECCs can be obtained by specialized crystallization under a high pressure of 300-500 MPa[18]).

In this study, high-power ultrasonication was utilized to induce SC_{OAF} in a uniaxially stretched PVDF homopolymer, and a hard-to-soft piezoelectric transition was successfully achieved. Namely, after ultrasonication, the PVDF sample exhibited higher piezoelectric

coefficients: d_{31} = 50.2±1.7 pm/V at room temperature (RT) and 76.2±1.2 pm/V at 65 °C. Moreover, the ultrasound-treated PVDF film exhibited good thermal stability up to 110 °C, which is comparable to the limit for piezoelectric $BaTiO_3$ ceramics (Fig. S1, ESI†). These stable high-temperature values of d_{31} are ~120% higher than any previously reported for neat PVDF.

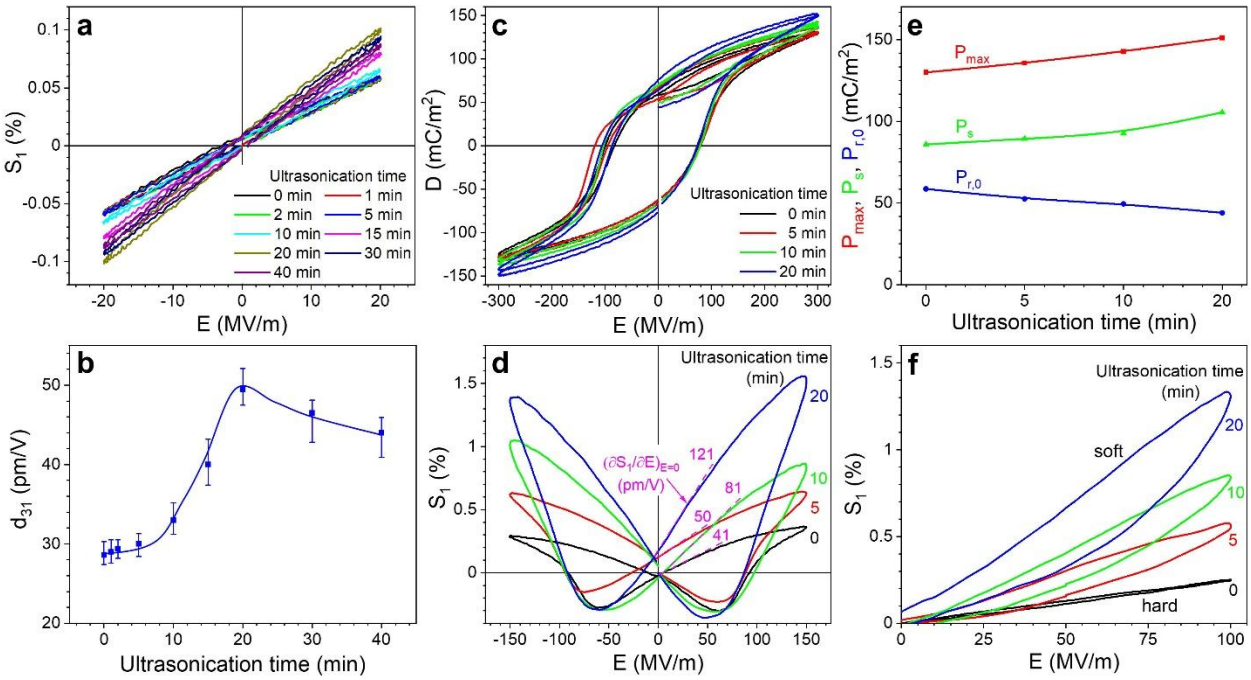

Fig. 1 (a) Low-field S_1-E loops for different PVDF-SPUx films (x indicates different lengths of ultrasonication time in minutes). (b) Calculated d_{31} values as a function of the ultrasonication time. (c) High-field bipolar first and second D-E loops and (d) second S_1-E loops for different PVDF-SPUx films. (e) P_{max}, P_s, and $P_{r,0}$ values obtained from the bipolar D-E loops in (c). (f) High-field unipolar S_1-E loops for different PVDF-SPUx films.

Results and discussion

Using an ultrasonication probe (pulsed at 300 W), the stretched and poled PVDF (PVDF-SP) was ultrasonicated for various lengths of time (see the Methods section), and the samples are denoted as PVDF-SPUx (x is the total ultrasonication time in minutes). The inverse piezoelectric coefficient d_{31} at RT was determined from the S_1-E loops in Fig. 1a, and d_{31} values are calculated from the linear slope: $S_1 = d_{31}E$ (Fig. 1b). Before ultrasound treatment, PVDF-SP showed a typical

d_{31} of 28.5±0.7 pm/V, which remained almost unchanged until rapidly increasing from 5 to 20 min of ultrasonication. A maximum value of 50.2±1.7 pm/V was seen at 20 min, after which d_{31} slightly decreased to 44.0±3.2 pm/V at 40 min.

To determine the cause of this behavior, high-field electric displacement-electric field (D-E) (Fig. 1c) and transverse strain-electric field (S_1-E) loops (Fig. 1d) were measured for different PVDF-SPUx films with x up to 20 min (note, high-field D-E loops could not be performed for x = 30 or 40 min, because defects induced by lengthy ultrasonication tended to cause easy dielectric breakdown). From the bipolar D-E loops in Fig. 1c, the maximum polarization (P_{max}), spontaneous polarization (P_s), and permanent remanent polarization ($P_{r,0}$, see refs. [21, 22] for the determination method) were extracted, and are summarized in Fig. 1e. Although P_{max} (from 129.9 to 151.1 mC/m^2) and P_s (from 85.8 to 105.5 mC/m^2) gradually increased with increasing ultrasonication time up to 20 min, $P_{r,0}$ continually decreased from 58.6 to 44.0 mC/m^2. This indicated that certain poled ferroelectric domains in the PVDF-SPU sample depolarized after ultrasonication. Meanwhile, the electro-elongation, i.e., S_1 in the positive direction, at 150 MV/m continuously improved with increasing the ultrasonication time (Fig. 1d). Generally, the piezoelectric coefficient could not be directly determined from the high-field poling loops due to the nonlinear ferroelectric switching. However, it is known that piezoelectricity is the electrostriction under a bias polarization.[23, 24] If the polarization persists during the return loop to E = 0, then the slope $(\partial S_1/\partial E)_{E=0}$ can be closely related to the piezoelectric performance. As can be seen in Fig. 1d, $(\partial S_1/\partial E)_{E=0}$ increased from 40.8 to 121.1 pm/V, suggesting enhancement in piezoelectricity upon ultrasonication.

Finally, a hard-to-soft piezoelectric transition was observed by measuring the unipolar S_1-E loops at 100 MV/m (slightly above the coercive field ~ 75 MV/m) (Fig. 1f). Without

ultrasonication, the PVDF-SP sample showed a linear S_1-E loop with a low hysteresis and the lowest actuation. This is typical hard-piezoelectric behavior. Upon increasing the ultrasonication time, the loop hysteresis became steadily larger, together with enhanced actuation, which is reminiscent of the typical soft-piezoelectric behavior. It is a new discovery that the piezoelectric coefficient is enhanced by the hard-to-soft transition for ferroelectric polymers.

Based on the above experimental results, we could infer that some of the originally poled dipoles in the PVDF-SP film became depolarized and thus mobile upon high-power ultrasonication. During subsequent electric poling of the PVDF-SPUx films, these polarizable dipoles contributed to piezoelectricity at low poling fields (Fig. 1a) and electroactuation under high poling fields (Fig. 1d). These newly generated polarizable dipoles should account for the observed hard-to-soft piezoelectric transition in Fig. 1f.

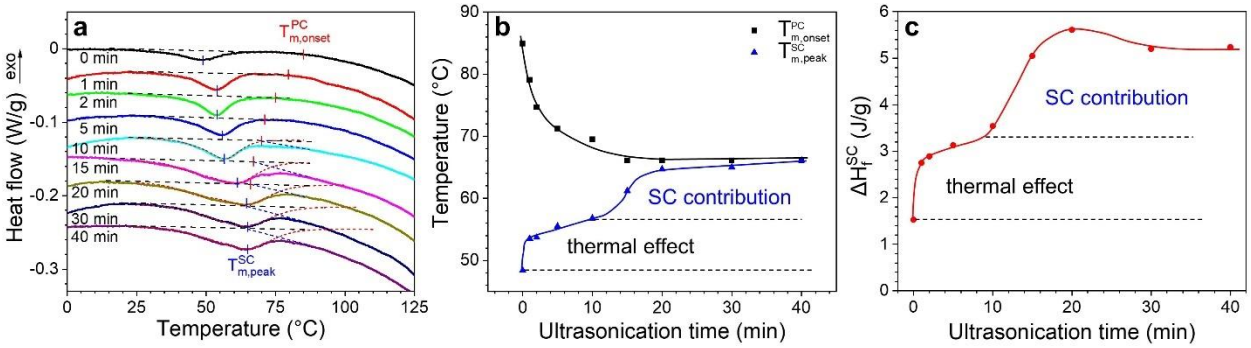

Fig. 2 (a) First-heating DSC curves from 0 to 125 °C. The heating rate is 10 °C/min. (b) $T^{SC}_{m,peak}$, $T^{PC}_{m,onset}$, and (c) ΔH_f^{SC} as a function of the ultrasonication time.

This raises the question of the origin of the polarizable dipoles induced by the high-power ultrasonication. To answer this question, structural [small-X-ray scattering (SAXS) and wide-angle X-ray diffraction (WAXD), Fig. S2-S4, ESI†] and thermal [differential scanning calorimetry (DSC), Fig. S5, ESI†] characterizations were performed. From the 2D SAXS patterns in Fig. S2 (ESI†), the crystalline lamellae were found to tilt ~60° from the stretching direction, and the tilt

angle did not change with ultrasonication. From Fig. S5a,b (ESI†), the overall lamellar spacing (determined by correlation function analysis in Fig. S6, ESI†) decreased slightly from 5.80 to 5.28 nm after ultrasonication for 40 min. In the 2D WAXD patterns in Fig. S4 (ESI†), an oriented β phase having its *c*-axis along the meridian (i.e., stretching) direction was observed for the PVDF-SPUx films. Using 2D WAXD analysis (Fig. S7, ESI†),[16] the contents of crystallinity (x_c), OAF/SC ($x_{OAF/SC}$), and IAF (x_{IAF}) were quantified (Fig. S5d, (ESI†). Up to 20 min ultrasonication time, x_c from PCs and x_{IAF} slightly decreased, and $x_{OAF/SC}$ slightly increased. No obvious difference in the $d_{110/200}$ spacing (~0.43 nm) was seen. In addition, Fourier transform infrared (FTIR) spectra of different PVDF-SPUx films are displayed in Fig. S8 (ESI†). All samples exhibited nearly identical spectra, showing the major ferroelectric β crystals with a trace amount of the nonpolar α phase. Based on these results, we conclude that the structural changes in response to high-power ultrasonication were too subtle to be clearly identified by SAXS, WAXD, and FTIR.

The full-range (-50 to 200 °C) DSC results are shown in Fig. S5a (ESI†). The T_m for the prime crystals (PCs) remained nearly constant at 156 °C, and the heat of fusion (ΔH_f^{PC}) slightly decreased from 44.1 J/g at x = 0 min to 41.1 J/g at x = 20 min (Fig. S5b, ESI†). Although no obvious difference could be identified for the PCs, observable changes were found for the minor melting peak at 50-60 °C (Fig. 2a). On the basis of prior reports,[22, 25] this weak melting peak was attributed to the SCs in PVDF. Using peak-fitting, the peak SC-melting ($T_{m,peak}^{SC}$) and the onset PC-melting ($T_{m,onset}^{PC}$) temperatures were determined, giving the results plotted in Fig. 2b. Before ultrasonication, the PVDF-SP film had a $T_{m,peak}^{SC}$ at 48.4 °C and a $T_{m,onset}^{PC}$ at 84.9 °C. After 1 min ultrasonication, the $T_{m,peak}^{SC}$ jumped to 53.5 °C. When the ultrasonication time increased to 15 min, another stepwise increase in $T_{m,peak}^{SC}$ was seen. Beyond 20 min, $T_{m,peak}^{SC}$ gradually reached a plateau around 65 °C. The $T_{m,onset}^{PC}$ continuously decreased and finally merged with $T_{m,peak}^{SC}$. In addition,

the heat of fusion for the SCs (ΔH_f^{SC}) was determined from the minor endothermic peaks in Fig. 2a, with the results shown in Fig. 2c. Similarly, two stepwise increases were also observed in ΔH_f^{SC}, consistent with the trend in $T_{m,peak}^{SC}$. Considering the high-energy input from ultrasonication, the first-step increase in $T_{m,peak}^{SC}$ and ΔH_f^{SC} could be attributed to a thermal annealing effect on SCs. The second-step increase can be attributed to an increased SC population. Judging from the second-step increase of ΔH_f^{SC} (2.4 J/g), the incremental amount of SCs should be very small, only ~0.025 (ΔH_f° is taken as 104.6 J/g[26]). This is the primary reason why structural characterization by SAXS and WAXD could not reveal significant changes after ultrasonication. Coincidentally, ΔH_f^{PC} decreased about 3.0 J/g after ultrasonication for 20 min (Fig. S5b, ESI†), nearly the same amount as the second-step increase of ΔH_f^{SC} (2.4 J/g). Meanwhile, the continuous decrease of the $T_{m,onset}^{PC}$ in Fig. 2b indicated damage to the PCs upon ultrasonication.

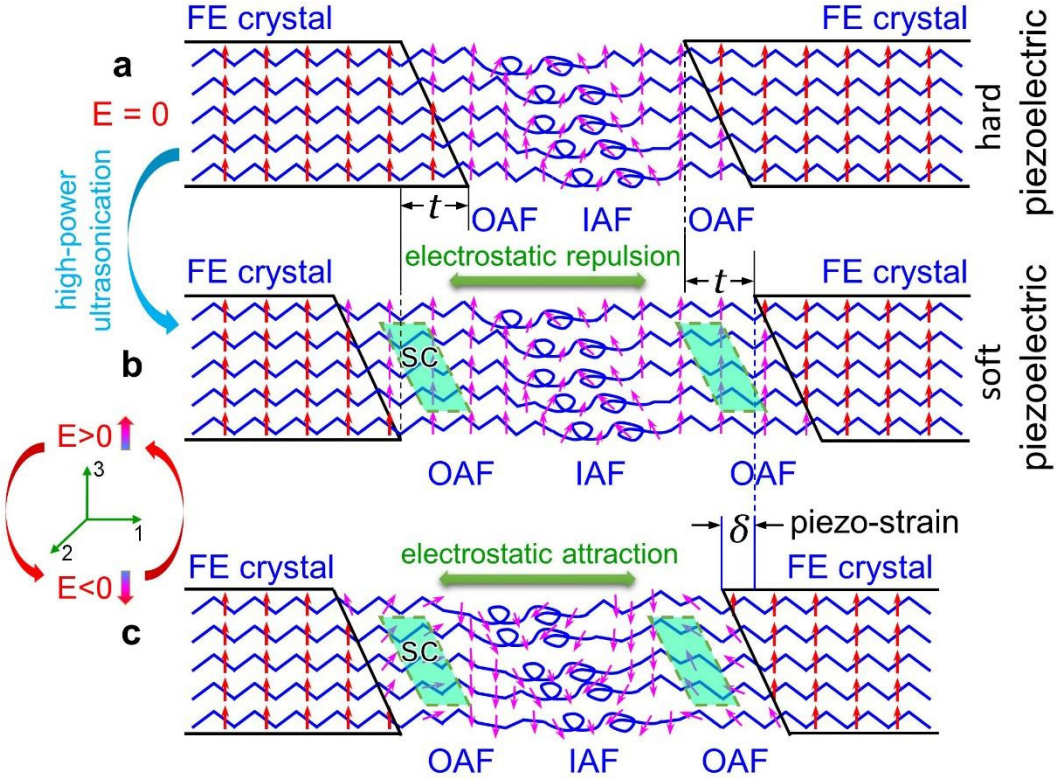

Fig. 3 Schematic SC/OAF formation by high-power ultrasonication and the inverse piezoelectricity in ferroelectric (FE) PVDF. (a) PVDF-SP at E = 0 and PVDF-SPUx at (b) E > 0 and (c) E < 0. Red and magenta arrows are the VDF dipoles in the poled β crystals and the amorphous phase (OAF + IAF), respectively. The green parallelograms in the OAF are SCs.

From these DSC results, we surmise that the high-power ultrasonication must have broken some surface layers (e.g., thickness t) off the PC lamellae and converted them into SCs (and possibly some OAF as well), as shown in the schematic representation in Fig. 3a,b. Because these broken-off SCs are located in the OAF at the crystal-amorphous interfaces, they could be the relaxor-like SC_{OAF} reported recently.[16] Intriguingly, this SC formation process coincides with the d_{31} increase from x = 5 to x = 20 min observed in Fig. 1b. It is likely that these new SCs broken off from the PCs are responsible for the enhanced d_{31} by ultrasonication and thus the hard-to-soft transition observed in Fig. 1f.

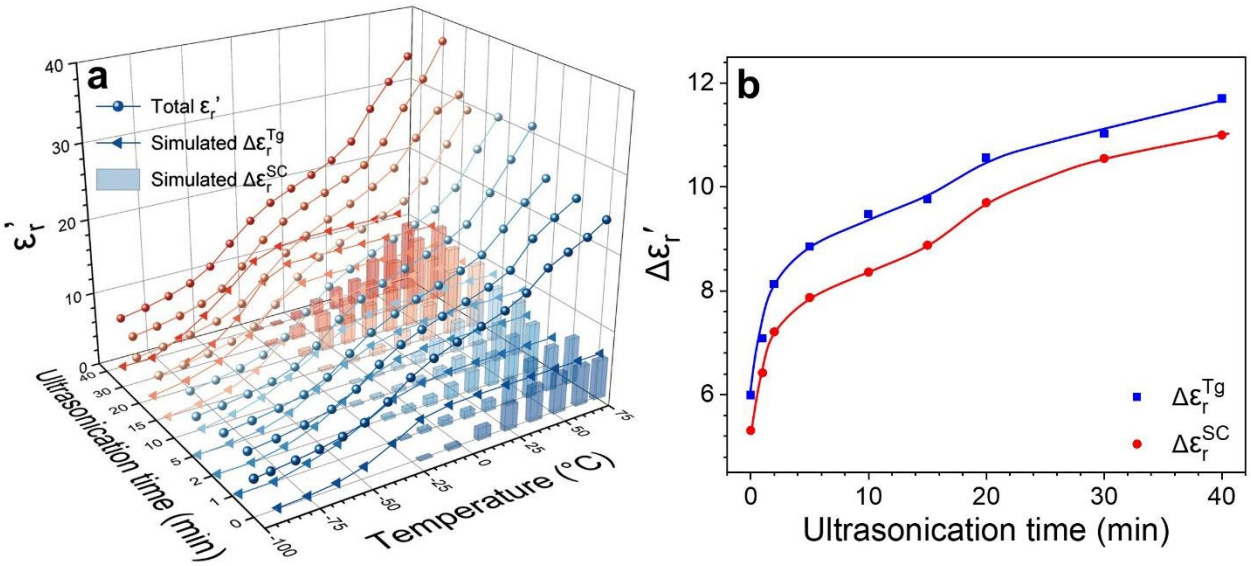

Fig. 4 (a) Temperature-scan BDS results, showing the total ε_r' and deconvoluted $\Delta\varepsilon_r^{Tg}$ and $\Delta\varepsilon_r^{SC}$. (b) Deconvoluted $\Delta\varepsilon_r^{Tg}$ and $\Delta\varepsilon_r^{SC}$ values as a function of the ultrasonication time.

Even though the hard-to-soft piezoelectric transition and the enhanced d_{31} are related to the newly formed SCs broken off from the PCs, there is still one open question: How did these SCs

induce the hard-to-soft transition and improve the piezoelectricity? To answer this question, temperature-scan broadband dielectric spectroscopy (BDS) measurements were performed (Fig. S6, ESI†). As recently reported,[17] BDS has the ability to detect the concentration and the rotational mobility of dipoles. Here, the real part of the relative permittivity (ε_r') at 1 Hz is chosen for further analysis (Fig. S7, ESI†). Three dielectric events were found from -100 to 150 °C, contributing to the stepwise increases in ε_r': glass transition temperature (T_g) at -35 °C, SC-melting (T_m^{SC}) around 60 °C, and ionic conduction above 75 °C. The multimode Havriliak-Negami (HN) formula was used for the deconvolution of the temperature-scan ε_r' (and ε_r'') curves,[27, 28] and results for the ε_r' are shown in Fig. S7 (ESI†). Contributions of the three dielectric events to the ε_r' were obtained: $\Delta\varepsilon_r^{Tg}$, $\Delta\varepsilon_r^{SC}$, and $\Delta\varepsilon_r^{Ion}$. The results for the PVDF-SPUx films are summarized in the three-dimensional plot in Fig. 4a. $\Delta\varepsilon_r^{Tg}$ and $\Delta\varepsilon_r^{SC}$ as a function of the ultrasonication time are shown in Fig. 4b. Both values increased after ultrasonication, and this is attributed to enhanced concentration and/or mobility of VDF dipoles in both the amorphous phase and SCs induced by ultrasonication. In this sense, these SCs should be the relaxor-like SC_{OAF}, as reported before.[16] Meanwhile, because the OAF makes a major contribution to the $\Delta\varepsilon_r^{Tg}$,[22, 25, 29-31] the increased $\Delta\varepsilon_r^{Tg}$ suggests an enhanced concentration and/or mobility of the dipoles in OAF.

Combining the results from the DSC (Fig. 2) and BDS (Fig. 4) studies, we propose the following mechanism for the hard-to-soft transition and improved piezoelectricity in the PVDF-SPUx films. High-power ultrasonication breaks the surface layers off the PC lamellae, increasing both concentrations and mobility of the dipoles in SCs and OAF (Fig. 3a,b). Meanwhile, these newly formed SCs and OAF largely depolarize, and thus decrease $P_{r,0}$ and increase P_s and P_{max}. Upon the application of an electric field E, these mobile SCs and OAF undergo both conformational transformation and electrostatic repulsion/attraction in the presence of the

remaining $P_{r,0}$ in the sample (Fig. 3b,c),[16] thus enhancing the piezoelectric performance. For example, when E > 0, the dipoles in the mobile OAF/SCs are oriented upward and the electrostatic repulsion among the parallel-aligned domains make the sample elongate along the stretching (i.e., 1) direction (Fig. 3b). When E < 0, the dipoles in the mobile OAF/SCs are oriented downward and the antiparallel-arranged domains induce electrostatic attraction, which shrinks the sample along the stretching direction (Fig. 3c). Meanwhile, these SCs and OAF become hysteretic during high-field unipolar poling, inducing the hard-to-soft piezoelectric transition seen in Fig. 1f.

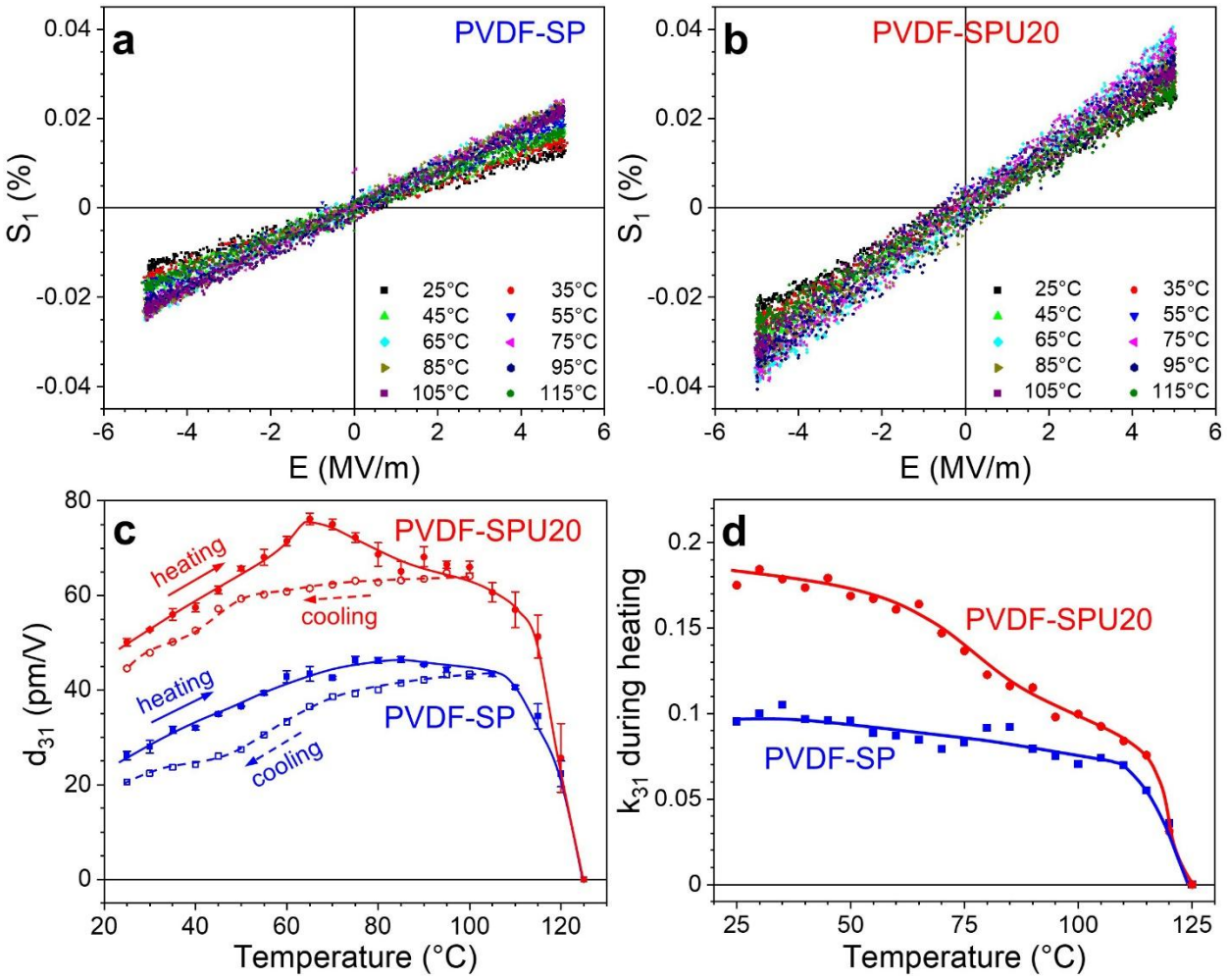

Fig. 5 Low-field S_1-E loops: (a) the PVDF-SP film and (b) the PVDF-SPU20 film at different temperatures. (c) Temperature-dependent d_{31} during the heating and cooling cycle. (d) Calculated k_{31} values during the heating process.

From the BDS results, the PVDF-SPUx films achieved a higher dielectric constant near T_m^{SC}, where the dipoles in the SCs underwent a temperature-activated process, similar to the behavior of SC_{OAF} reported in the low-VDF-content P(VDF-TrFE) films.[16] It is thus expected that the d_{31} could be further enhanced at elevated temperatures. Fig. 5a,b show low-field S_1-E loops for the PVDF-SP and the PVDF-SPU20 films, respectively. Indeed, the maximum d_{31} of 76.2 pm/V was achieved at 65 °C for the PVDF-SPU20, which was around the T_m^{SC} (Fig. 5c). After the SCs melted, the d_{31} at 100 °C dropped to 61.0 pm/V. At temperatures above 100 °C, PVDF started to lose the $P_{r,0}$ via a thermally activated depolarization process.[22, 32] Finally, the piezoelectricity totally disappeared around 125 °C. When we stopped heating at 100 °C followed by cooling, the d_{31} continuously decreased without any maximum point around 65 °C. This is because the ultrasonication-induced SCs had already melted. Even though the SCs melted, they transformed into mobile OAF, which still helped to maintain high piezoelectricity.[21] For the PVDF-SP film, the increase in d_{31} upon heating was less pronounced, as compared to the PVDF-SPU20 film, because it did not have the relaxor-like SCs. The d_{31} started to decrease around 110 °C, and finally the piezoelectricity disappeared, again around 125 °C. During cooling, d_{31} gradually decreased with decreasing temperature. In addition, the electromechanical coupling factor k_{31} was obtained by measuring the dielectric constant at 1 kHz (Fig. S6, ESI†) and Young's (or tensile) modulus (Y_1) (Fig. S8, ESI†): $k_{31} = d_{31}(Y_1/\varepsilon_r\varepsilon_0)^{0.5}$,[23] where ε_0 is the vacuum permittivity. The calculated k_{31} values for the PVDF-SP and PVDF-SPU20 films are shown in Fig. 4d. The highest k_{31} values for the PVDF-SPU20 and PVDF-SP films were 0.18 and 0.11, respectively. Upon heating, both values monotonically decreased and finally became zero around 125 °C.

During manuscript revision, a question was raised regarding the effect of thermal annealing

on piezoelectric performance of the PVDF films. It was reported that thermal annealing of P(VDF-TrFE) 45/55 at 90 °C could lead to disappearance of the ferroelectric phase and promote the relaxor ferroelectric phase, leading to enhanced dielectric constant.[33] However, thermal annealing of PVDF at high temperatures would lead to an opposite effect. To demonstrate the thermal annealing effect, the stretched PVDF film was annealed at 120 °C for 2 days, followed by unidirectional electric poling at 400 MV/m for 40 times (10 Hz) to achieve the macroscopic dipole moment. The sample is denoted as PVDF-SAP. As shown in Figs. S13a,b (ESI†), the ΔH_f^{PC} increased significantly from 44.1 J/g for PVDF-SP to 56.7 J/g for PVDF-SAP, indicating an increase of crystallinity. The dielectric constant at room temperature and 10 Hz dropped from 15.1 for PVDF-SP to 11.7 for PVDF-SAP (Fig. S13c, ESI†). Finally, the d_{31} decreased to around 15 pm/V (Figs. S13e,f, ESI†), significantly lower than those (50.2-76.2 pm/V) of the PVDF-SPU20 film. The reason for the decreased piezoelectric performance of the PVDF-SAP film was unraveled by an in-situ heating study using synchrotron SAXS and WAXD. As shown in Fig. S14a-c (ESI†), the overall lamellar thickness continuously increased from 5.75 nm for PVDF-SP to 8.85 nm for PVDF-SPA, and the $d_{110/200}$ decreased from 0.4255 nm for PVDF-SP to 0.4224 nm for PVDF-SPA during heating to 120 °C, indicating a tighter crystalline packing upon thermal annealing. Finally, using 2D WAXD analysis, x_c increased from 0.431 for PVDF-SP to 0.560 for PVDF-SPA, and $x_{OAF/SC}$ and x_{IAF} decreased from 0.285 and 0.284 for PVDF-SP to 0.221 and 0.219 for PVDF-SPA (Fig. S14d, ESI†). It is the tighter crystal-packing and decreased $x_{OAF/SC}$ that caused the significant decrease of piezoelectric performance for thermally annealed PVDF film.

In summary, high-power ultrasonication has been shown to be an effective way to generate mobile SCs and OAF in the hard-piezoelectric PVDF-SP film, most likely by breaking off surface layers from the PC lamellae. From the DSC study, the volume fraction of the newly generated SCs

was estimated to be ~0.025. Although this amount was small, these SCs were relaxor-like as evidenced by the temperature-scan BDS result. These highly polarizable SCs and OAF, broken off from the PCs by ultrasonication, induced a hard-to-soft piezoelectric transition, and thus enhanced the d_{31}. Upon heating, a maximum d_{31} of 76.2±1.2 pm/V was achieved at 65 °C. A high d_{31} ~ 60 pm/V persisted up to 110 °C. In a comparison with other piezoelectric polymers and composites, the piezoelectric performance, in terms of maximum d_{31} and usage temperature, is the highest for the ultrasound-treated PVDF-SPU20 film, and is similar to that of piezoelectric $BaTiO_3$ (Fig. S1, ESI†). This work not only demonstrates the effect of relaxor-like SC_{OAF} and OAF on improving the piezoelectric performance of polymers, but also indicates a promising pathway for the design and fabrication of commercially viable products for various electromechanical applications. For example, we recently discovered that multistep uniaxial stretching of the hot-pressed PVDF films could also achieve a high d_{31} of 50 pm/V at room temperature (Fig. S15, ESI†). Detailed results will be reported in the future.

Acknowledgements

This work is supported by the National Science Foundation, Division of Materials Research, Polymers Program (DMR-2103196). This research used the 11-BM CMS beamline of National Synchrotron Light Source II (NSLS-II), Brookhaven National Laboratory (BNL), a U.S. Department of Energy User Facility operated for the Office of Science by BNL under contract DE-SC0012704. E.A. also acknowledges the support by the Ministry of Science and Higher Education of the Russian Federation (State Assignment No. 075-01056-22-00).

Conflict of interest

The authors declare no competing financial interests.

References

[1] B. Jaffe, W. R. Cook and H. L. Jaffe, *Piezoelectric Ceramics*, Academic Press, London, New York, 1971.

[2] T. R. Shrout and S. J. Zhang, *J. Electroceramics* 2007, **19,** 111-124.

[3] F. Li, L. Wang, L. Jin, D. Lin, J. Li, Z. Li, Z. Xu and S. J. Zhang, *IEEE Trans. Ultrason. Ferroelectr. Freq. Control* 2015, **62,** 18-32.

[4] M. G. Broadhurst, G. T. Davis, J. E. Mckinney and R. E. Collins, *J. Appl. Phys.* 1978, **49,** 4992-4997.

[5] K. Tashiro, M. Kobayashi, H. Tadokoro and E. Fukada, *Macromolecules* 1980, **13,** 691-698.

[6] Y. Wada and R. Hayakawa, *Ferroelectrics* 1981, **32,** 115-118.

[7] T. Furukawa, J. X. Wen, K. Suzuki, Y. Takashina and M. Date, *J. Appl. Phys.* 1984, **56,** 829-834.

[8] M. G. Broadhurst and G. T. Davis, *Ferroelectrics* 1984, **60,** 3-13.

[9] T. Furukawa and N. Seo, *Jpn. J. Appl. Phys.* 1990, **29,** 675-680.

[10] S. Tasaka and S. Miyata, *Ferroelectrics* 1981, **32,** 17-23.

[11] A. Strachan and W. A. Goddard, *Appl. Phys. Lett.* 2005, **86,** 083103.

[12] Y. Liu, H. Aziguli, B. Zhang, W. Xu, W. Lu, J. Bernholc and Q. Wang, *Nature* 2018, **562,** 96-100.

[13] Y. Liu and Q. Wang, *Adv. Sci.* 2020, **7,** 1092468.

[14] P. Harnischfeger and B. J. Jungnickel, *Ferroelectrics* 1990, **109,** 279-284.

[15] I. Katsouras, K. Asadi, M. Li, T. B. van Driel, K. S. Kjaer, D. Zhao, T. Lenz, Y. Gu, P. M. Blom, D. Damjanovic, M. M. Nielsen and D. M. de Leeuw, *Nat. Mater.* 2016, **15,** 78-84.

[16] Z. Zhu, G. Rui, Q. Li, E. Allahyarov, R. Li, T. Soulestin, F. Dos Santos, H. He, P. Taylor and L. Zhu, *Matter* 2021, **4,** 3696-3709.

[17] Z. Zhu, G. Rui, R. Li, H. He and L. Zhu, *Macromolecules* 2021, **54,** 9879-9887.

[18] T. Hattori, M. Hikosaka and H. Ohigashi, *Polymer* 1996, **37,** 85-91.

[19] T. Hattori, M. Kanaoka and H. Ohigashi, *J. Appl. Phys.* 1996, **79,** 2016-2022.

[20] T. Hattori, T. Watanabe, S. Akama, M. Hikosaka and H. Ohigashi, *Polymer* 1997, **38,** 3505-3511.

[21] Y. Huang, G. Rui, Q. Li, E. Allahyarov, R. Li, M. Fukuto, G. Zhong, J. Xu, Z. Li, P. L. Taylor and L. Zhu, *Nat. Commun.* 2021, **12,** 675.

[22] G. Rui, Y. Huang, X. Chen, R. Li, D. Wang, T. Miyoshi and L. Zhu, *J. Mater. Chem. C* 2021, **9,** 894-907.

[23] Q. M. Zhang, C. Huang, F. Xia and J. Su, in *Electroactive Polymer (EAP) Actuators as Artificial Muscles: Reality, Potential, and Challenges,* 2nd ed., SPIE Press, 2004, Chapter 4, pp 89-139.

[24] F. Li, L. Jin, Z. Xu and S. J. Zhang, *Appl. Phys. Rev.* 2014, **1,** 011103.

[25] L. Yang, J. Ho, E. Allahyarov, R. Mu and L. Zhu, *ACS Appl. Mater. Interfaces* 2015, **7,** 19894-19905.

[26] K. Nakagawa and Y. Ishida, *J. Polym. Sci., Part B: Polym. Phys.* 1973, **11,** 2153-2171.

[27] X. Chen, E. Allahyarov, Q. Li, D. Langhe, M. Ponting, D. Schuele, E. Baer and L. Zhu, *Compos. B: Eng.* 2020, **190,** 107908.

[28] X. Chen, E. Allahyarov, D. Langhe, M. Ponting, R. Li, M. Fukuto, D. Schuele, E. Baer and L. Zhu, *J. Mater. Chem. C* 2020, **8,** 6102-6117.

[29] B. Hahn, J. Wendorff and D. Y. Yoon, *Macromolecules* 1985, **18,** 718-721.

[30] B. R. Hahn, O. Herrmannschonherr and J. H. Wendorff, *Polymer* 1987, **28,** 201-208.

[31] B. Lu, K. Lamnawar, A. Maazouz and H. G. Zhang, *Soft Matter* 2016, **12,** 3252-3264.

[32] J. Jones, L. Zhu, N. Tolk and R. Mu, *Appl. Phys. Lett.* 2013, **103,** 072901.

[33] S. Nayak, H. T. Ng and A. Pramanick, *Appl. Phys. Lett.* 2020, **117**, 232903.